

3D welding and milling: Part I—a direct approach for freeform fabrication of metallic prototypes

Yong-Ak Song^{a,*}, Sehyung Park^a, Doosun Choi^b, Haesung Jee^c

^a*Korea Institute of Science and Technology KIST, CAD/CAM Research Center, P.O. Box 131, Cheongryang, Seoul, South Korea*

^b*Korea Institute of Machines and Materials KIMM, 171 Jang-Dong, Yusong-Gu, Taejeon, South Korea*

^c*Hongik University, Department of Mechanical Engineering, 72-1, Sangsu-Dong, Mapo-Gu, Seoul, South Korea*

Received 4 August 2004; accepted 19 November 2004

Available online 11 January 2005

Abstract

Solid Freeform Fabrication (SFF) gives engineers a new freedom to build parts that have thus far proved difficult to manufacture using conventional machining. However, the surface finish and accuracy of SFF parts are lower than those of conventionally machined parts. A process combination of additive and subtractive techniques is currently being developed in order to overcome this problem. A novel hybrid approach of our group called ‘3D welding and milling’ uses gas metal arc welding as an additive and milling as a subtractive technique, thereby exploiting the advantages of both processes. Compared to other deposition processes, gas metal arc welding is the most economic way of depositing metals. In this paper, the initial results of the process development and the characterization of the parts fabricated by this process are reported.

© 2004 Elsevier Ltd. All rights reserved.

Keywords: Solid Freeform Fabrication (SFF); Rapid Prototyping; Gas metal arc welding (GMAW); Milling

1. Introduction

With an increasing demand for metallic prototypes and tools [1], several direct SFF techniques such as 3D Welding [2], Selective Laser Sintering (SLS) [3], Laser-Engineered Net Shaping (LENS) [4], Directed Light Fabrication (DLF) [5], Direct Metal Deposition (DMD) [6], Controlled Metal Buildup (CMB) [7], Shape Deposition Manufacturing (SDM) [8], and more recently, Precision Metal Deposition (PDM) [9] have been developed. The feature common to all of these approaches is that metals, either in the form of powder or wire, are melted directly with an arc or laser beam. Due to the complete melting, however, the accuracy and surface quality of the parts are generally lower than those of machined parts.

Among the above-mentioned processes, SDM of Stanford University and CMB developed at the IPT Aachen use

a combination of additive and subtractive techniques to accomplish the deposition and the machining processes in the same setup. In these processes, each layer is deposited as a near net shape using laser cladding. The layer is then shaped in a CNC milling operation to a net shape before proceeding with the next layer. In SDM processes, the top as well as the side faces of each layer are machined and then protected by a support structure made of copper. This support structure is then removed in an etching process when the part is completely fabricated.

The combination of welding as an additive and milling as a subtractive process can provide distinctive advantages over conventional machining. Firstly, if a large volume must be removed, the fabrication of a near-net-shape part using the additive method and the subsequent surface finishing can offer a competitive approach in terms of fabrication time. In addition, if the material is difficult to machine, the additive fabrication of a near net shape part offers an economic way to machine it because of less tool wear. Secondly, features that are either impossible or difficult to machine can be manufactured using the hybrid approach.

* Corresponding author. Tel.: +1 617 253 8516; fax: +1 617 258 5846.
E-mail address: yongak@mit.edu (Y.-A. Song).

¹ Currently affiliated with Massachusetts Institute of Technology.

Nomenclature

P	welding power (W)	v_m	milling speed (m/min)
U	welding voltage (V)	h_s	bead offset (mm)
I	welding current (A)	t	layer thickness (mm)
v_s	welding speed (m/min)		

Such features include deep and narrow slots as well as arbitrary internal structures such as conformal cooling channels [10]. Thirdly, the combined process permits fabricating accurate parts with various materials, depending on the functional requirements [11].

As a new hybrid solid freeform fabrication process, gas metal arc welding (GMAW) is combined with conventional milling to directly fabricate metallic prototypes. This report focuses on the identification of the basic process characteristics and the characterization of the fabricated parts in order to see whether the process can be successfully applied to the manufacture of functional parts, especially tools.

2. Process principle and experimental setup of 3D welding and milling

The principle of the 3D welding and milling process is based on the layered deposition of molten wire material using GMAW, which is the most economic way of depositing molten metals. However, its beads are of lower quality than laser welding beads with respect to accuracy and surface quality. Since a post-processing step, e.g. surface machining, is required for most of the parts built by direct deposition approaches, the relatively low accuracy and surface quality of arc-welded beads is acceptable. GMAW also offers a distinct technical advantage with regard to the possibility of vertical wire feeding: the welding result is independent from the change of the relative movement between the wire nozzle and the x - y table.

Fig. 1 shows the process principle of 3D Welding and Milling. First, a layer is built by depositing single beads side by

side with bead offset h_s . Depending on the welding parameters such as welding speed v_s and welding power P , the bead thickness t varies between 0.5 and 1.5 mm. The distance between single beads h_s is an important process parameter determining the overlapping of beads and thereby the layer's surface quality. When deposited, the top surface of the layer is machined to a prescribed thickness for further deposition.

Combining the deposition with subsequent face milling enables us to make changes in the layer thickness between 0.1 and 1 mm. This is, in fact, a unique feature of the process in that an adaptive slicing with variable layer thickness is enabled. When the sequence of deposition and face milling is finished, surface finishing is applied in the same setup to remove remaining stair steps on the surface. Any dimensional and geometrical inaccuracy resulting from the deposition can be completely compensated for by this final surface finishing.

The experimental setup for the 3D Welding and Milling process is shown in Fig. 2. The setup is based on a 3-axis milling machine with two welding guns that are vertically attached to the spindle housing. A simple retrofitting of a common 3-axis milling machine is required in order to carry out the process, thus eliminating any need to buy special equipment such as linear axes. The two welding guns allow switching between two different wire materials or between two different wire material sizes. On the left side of the spindle, a laser welding head is attached to enable testing of an alternative deposition method. The single beads are deposited on a substrate plate, which is preheated up to 200 °C with a built-in heater. The preheating of the substrate plate is used to reduce the thermal stress buildup during deposition.

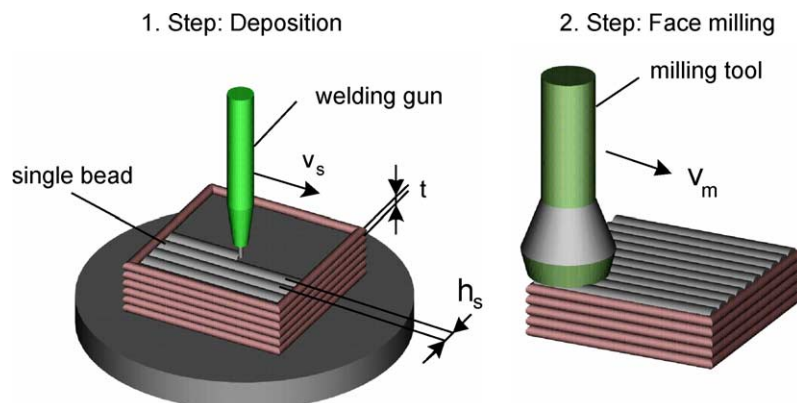


Fig. 1. Process principle of 3D Welding and Milling.

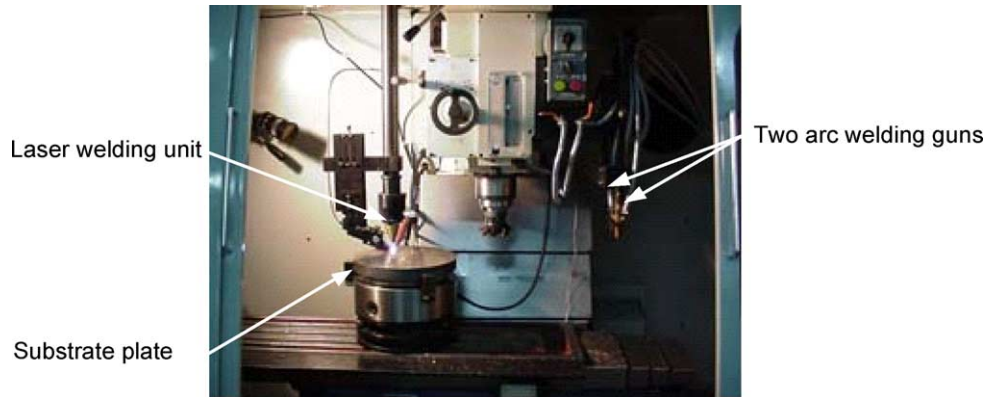


Fig. 2. View of 3D welding and milling machine.

According to the process data flow shown in Fig. 3, the STL file is sliced at a prescribed layer thickness in the ‘CyberRP’, a self-developed STL editor for pre-processing STL files, shown in Fig. 4. Any number of parts can be loaded as long as these fit in the machine and then are verified. This step is helpful in finding and fixing errors in the STL files. Typically, errors in a STL file include inconsistent normal directions of a triangle and small cavities in the part. Later, the parts are either automatically or manually positioned in the 3D build space, and support structures are generated for all parts. Supports are generated automatically, though these can be modified manually if required. After editing and slicing of the STL file, the Common Layer Interface (CLI) file is obtained which contains the polygon data of each layer.

Following the slicing step, the CLI file is imported into the NC post-processing software, ‘RapidNC’, which generates a NC tool path for filling the inner area as well as

the contour of each layer after selecting the bead offset h_s and the welding speed v_s . The software database allows the selection of optimal process parameters depending on the wire material and the diameter. It also enables the use of different building strategies such as deposition with and without alternating the filling direction between each layer. As for the layer filling technique, one-way and zigzag tool paths are offered.

3. Experimental investigation and results

3.1. Deposition parameters

Starting from the single bead experiment, the influence exerted by the main process parameters, welding voltage U , welding current I , and welding speed v_s on the deposition of single beads was investigated. The wire material used was a mild steel AWS 5.18 70S-6 with a 0.9 mm diameter. Optimizing the welding parameters in the ranges of $U=16\text{--}36\text{ V}$ and $I=60\text{--}140\text{ A}$ at a welding speed between $v_s=0.2$ and $v_s=1.4\text{ m/min}$, permitted the deposition of

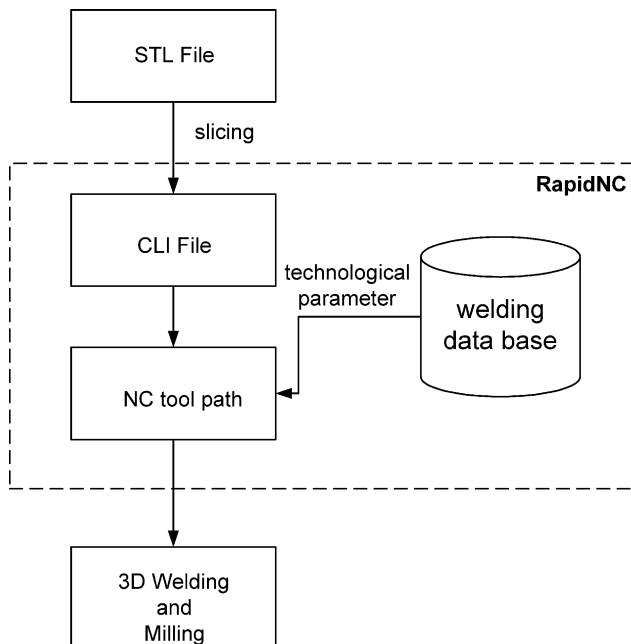


Fig. 3. Preparation of the process data with ‘RapidNC’.

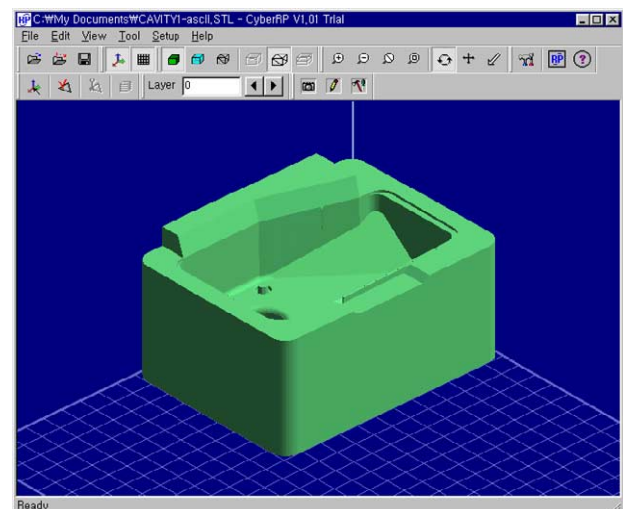


Fig. 4. GUI of the STL editor ‘CyberRP’.

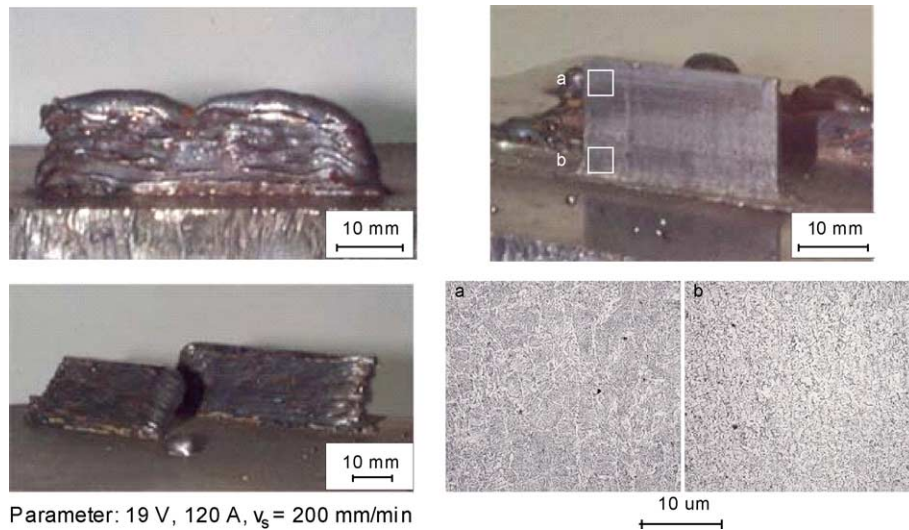


Fig. 5. Thin-walled part before and after machining.

single, connected beads. Based on this result, the welding parameters for all the following depositions were set to $U = 19$ V and $I = 120$ A with a welding speed of $v_s = 1.2$ m/min.

3.2. Fabrication and characterization of test parts

When stacking the beads on each other, the heat accumulation influences the deposition in terms of layer thickness. For this reason, it is necessary to vary the process parameters depending on the actual thickness of the deposited layer. Such a parameter control, however, requires an elaborate on-line temperature or height measurement, which makes the entire system more

complex. In our process, the variation of thickness in each layer is simply compensated by face milling after each deposition. In case of a thin wall consisting of eight layers with a layer thickness of $t = 0.8$ mm, a wall thickness of 4 mm was achieved with a surface roughness of $R_a = 150$ μm along the height, as shown in Fig. 5. Fig. 5 also shows two inclined walls with a bead offset of $h_s = 0.5$ and 1 mm, respectively. This shows that even without using a special support structure, an inclination of the layers up to 45° is possible.

After machining, a wall thickness of 1 mm was obtained with a surface roughness of $R_a = 2$ μm . Analysis of the cross-section in the vertical wall reveals different

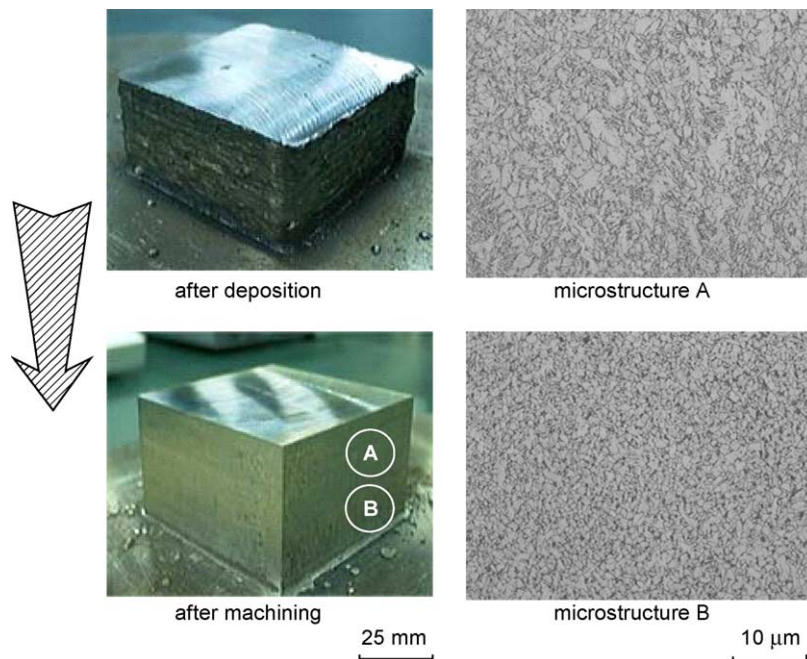


Fig. 6. Solid test part before and after machining with its microstructures.

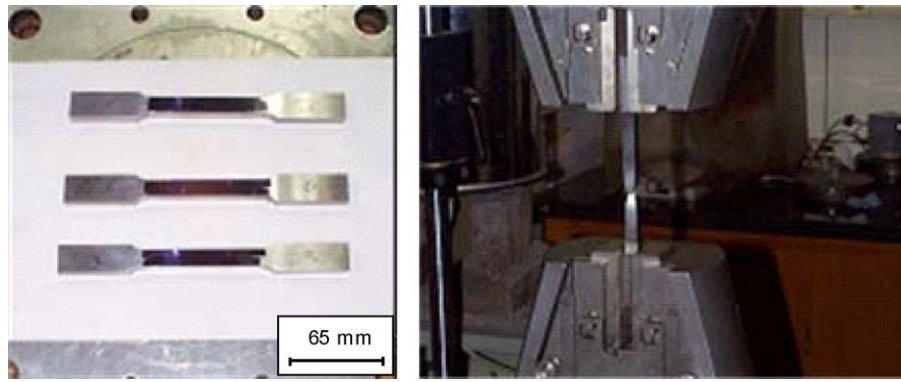


Fig. 7. Freeform-fabricated tensile test specimens.

microstructures, depending on the height of the measurement location along the wall. The microstructure on the upper area of the wall contains enlarged grains with a spherical shape (see Fig. 5a). In each grain, a second phase can be observed, which indicates a relatively low cooling rate in the upper part of the wall. In comparison, the microstructure of the lower part contains relatively small grains and some dendrites (see Fig. 5b). A microstructure of this nature is the result of rapid cooling, which, in our case, is caused by the high rate of heat conduction from the lower part of the wall into the substrate plate.

Besides thin-walled parts, solid parts can also be built when an appropriate bead offset h_s is selected between single beads. As shown in Fig. 6, a rectangular solid was built with a layer thickness of $t=0.8$ mm while alternating the deposition direction between each layer. The optimized bead offset was $h_s=2.8$ mm. The measurement shows a dimensional accuracy of the solid test part within ± 0.5 mm which was increased to 20 μm with a surface quality of $R_a=2$ μm after machining.

The microstructure analysis shows an almost completely dense structure of the solid test part. Only a small number of process-inherent pores are recognizable in the microstructure. This dense structure is due to the fact that most of the pores, normally existing in the overlapping zone between the beads, are completely removed during face milling. Similar to the microstructure of the wall, analysis of

the cross-section in the rectangular solid also yields a difference in microstructure along the height. The microstructure of the upper area of the solid contains enlarged grains with some dendrites (see microstructure A in Fig. 6), whereas the lower area has relatively small grains (see microstructure B in Fig. 6). The hardness measurement proves that there are different microstructures along the height of the rectangular solid. Starting from a hardness value of 331.8 HV at the bottom of the part, this measurement decreases gradually to 280.5 HV as the height increases.

The applicability of 3D welding and milling for the prototyping of functional prototypes or tools depends mainly on the mechanical strength of the parts. In order to assess the mechanical strength, rectangular tension test specimens are made and tested according to the ASTM specification, as shown in Fig. 7. As for the building technique, the beads are deposited in the direction of the applied tension. The values, measured parallel to the building direction, are 620 MPa, whereas the mild steel as wire material has a tensile strength of 550 MPa. This result proves that the tensile strength of the multiple-welded structure is comparable to that of conventional mild steel. This value also corresponds to the tensile strength of EOS DMLS Direct Steel 20-V1 or stainless steel 1.4404 built with Selective Laser Melting (SLM) [12]. In Table 1, the currently achievable specifications of 3D welding and Milling are summarized in comparison with the SLS and LENS processes.

Table 1
Comparison of 3D welding and milling process with SLS and LENS

	SLS [12]	LENS [4, 12]	3D Welding and Milling
Density	~60% raw	>90%	>90%
Accuracy	~0.1 mm	>0.1 mm	± 0.5 mm (without milling) \rightarrow ± 0.01 mm (with milling)
Surface roughness R_a	20–40 μm before infiltration, 10–15 μm after infiltration	6.35 μm [4]	150 μm (without milling) \rightarrow 2 μm (with milling)
Mechanical strength (MPa)	600	790 [4]	620

4. Conclusions

At present, the dimensional accuracy as well as the surface quality of metallic parts and tools manufactured using SFF techniques still lag far behind those of conventionally machined parts. To increase accuracy as well as surface quality, a hybrid approach called 3D welding and milling has been developed which exploits the advantages of additive and subtractive techniques.

The accuracy and surface quality before machining are low compared to the other commercialized processes with

$< \pm 0.5$ mm and $150\text{ }\mu\text{m}$, respectively. This can be increased, however, with subsequent surface finishing in the same setup. The microstructure is dense with a microhardness value of 330 HV. The tensile strength achieved was 620 MPa, which is comparable to the values obtained with other direct metal deposition processes.

The successful fabrication of metallic parts demonstrates the potential of the 3D Welding and Milling process for prototyping and tooling. Further studies, however, must examine how this process is competitive compared with the conventional milling operations in terms of manufacturing time. To gain competitiveness, further studies should concentrate on increasing the deposition speed as well and accuracy of the deposited beads.

References

- [1] A. Rosochowski, A. Matuszak, Rapid tooling: the state of the art, *Journal of Materials Processing Technology* 106 (2000) 191–198.
- [2] P.M. Dickens, M. Pridham, R. Cobb, I. Gibson, G. Dixon, 3D welding, in: *Proceedings of the First European Conference on Rapid Prototyping*, University of Nottingham, England, pp. 81–93.
- [3] M. Khaing, J. Fuh, L. Lu, Direct metal laser sintering for rapid tooling: processing and characterization of EOS parts, *Journal of Materials Processing Technology* 113 (2001) 269–272.
- [4] M. Griffith et al., Freeform fabrication of metallic components using laser engineered net shaping (LENS), in: *Proceedings of the Solid Freeform Fabrication Symposium*, University of Texas at Austin, 1996, pp. 125–131.
- [5] G. Lewis, J. Milewski, D. Thoma, Properties of near-net shape metallic components made by the direct light fabrication process, in: *Proceedings of the Solid Freeform Fabrication Symposium*, University of Texas at Austin, 1997, pp. 513–520.
- [6] J. Mazumder, J. Choi, K. Nagarathnam, J. Koch, D. Hetzner, The direct metal deposition of H13 tool steel for 3D components. *Journals of the Minerals, Metals and Materials* 1997: 49 (5) 55–60.
- [7] C. Freyer, F. Klocke, Fast manufacture of high strength tools from steel using CMB, in: *Proceedings of SME Conference Rapid Prototyping and Manufacturing*, Cincinnati (OH), 14–17 May, 2001.
- [8] J.R. Fessler, R. Merz, A. Nickel, F. Prinz, Laser deposition of metals for shape deposition manufacturing, in: *Proceedings of the Solid Freeform Fabrication Symposium*, University of Texas at Austin, 1996, pp. 117–124.
- [9] J. Rabinovich, Laser precision metal deposition PMD, in: *Proceedings of the SME Conference Rapid Prototyping and Manufacturing*, Cincinnati (OH), 30 April–2 May, 2002.
- [10] X. Xu, E. Sachs, S. Allen, M. Cima, Designing conformal cooling channels for tooling, in: *Proceedings of the Solid Freeform Fabrication Symposium*, University of Texas at Austin, 1998, pp. 131–146.
- [11] M. Griffith, L. Harwell, J. Romero, E. Schlienger, C. Atwood, J. Smugeresky, Multi-material processing by LENS, in: *Solid Freeform Fabrication Proceedings*, University of Texas at Austin, 1997, pp. 387–394.
- [12] G. Levy, R. Schindel, J.P. Kruth, Rapid manufacturing and rapid tooling with layer manufacturing (LM) technologies, state of the art and future perspective, *CIRP Annals* 52/2 (2003) 589–609.